

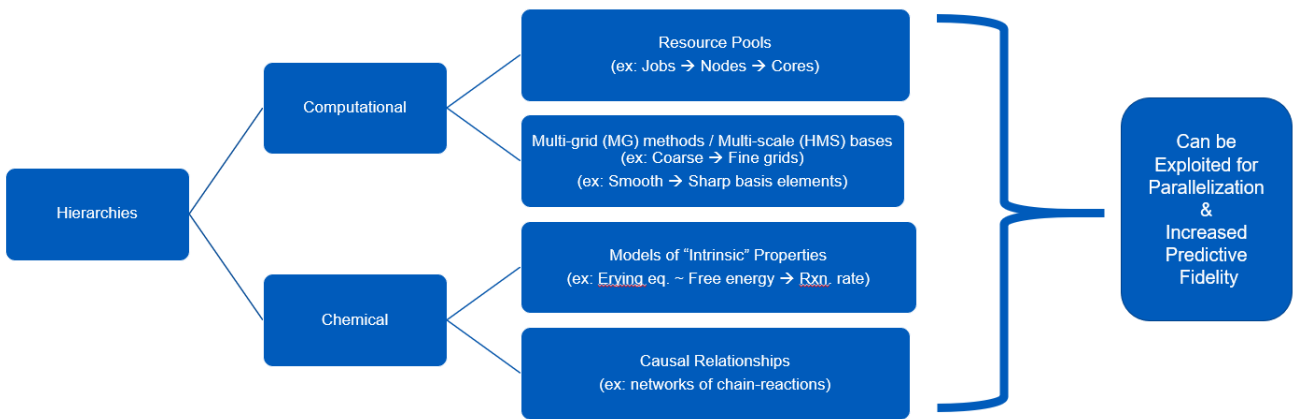
# A Hierarchical Perspective on Computational Chemistry: Parallelization and Predictive Fidelity, with “Old Toys” and “New Tricks”

Alex Becerra

December 22, 2023

## Abstract

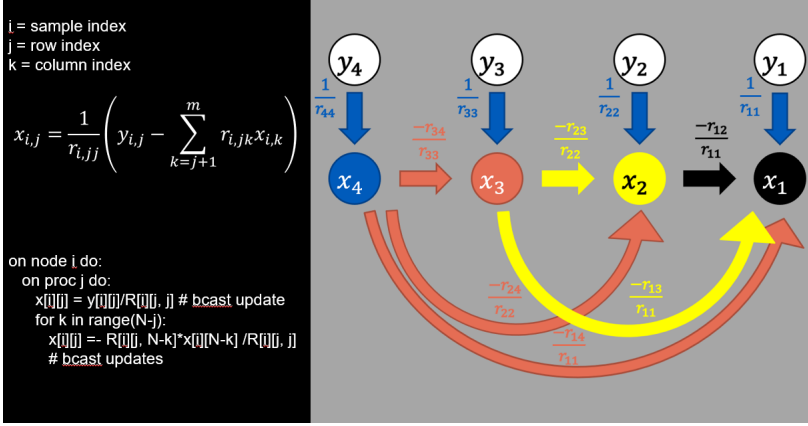
Most broadly, this paper discusses how both hierarchies of a computational nature and hierarchies of a chemical nature can be exploited for efficient parallelism and increased predictive fidelity. While the examples presented here focus primarily on applications to the field of computational chemistry, the underlying concepts extend beyond to modeling many kinds of physical systems. More specifically, the core result of this paper is the development of a “new trick” (recursive Kronecker/Pauli decompositions) for an “old toy” (estimating the energy levels for a particle in a ring via FDM/MG). Further connections, discussion, examples, and motivation are provided to leave the reader with the notion that this is a versatile trick that is compatible with many existing computational frameworks as well as the notion that even this toy example has many practical uses.



## 1 Introduction

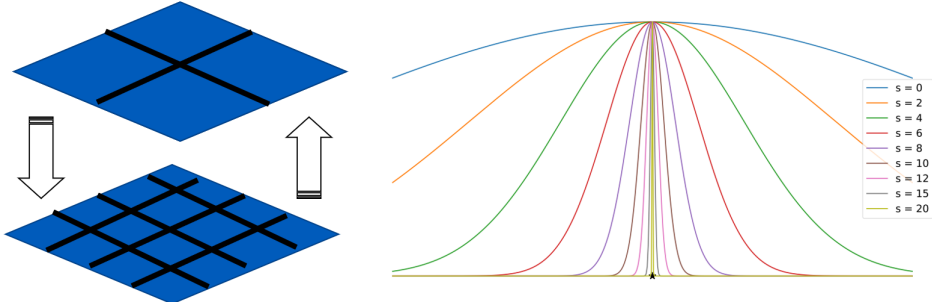
Firstly, we set out to provide a concrete sense of some different kinds of hierarchies and some different ways that they can be exploited. We shall make a distinction between hierarchies of a computational nature and hierarchies of a chemical nature by providing 2 relevant examples of each.

## 1.1 Computational Hierarchy



via back-substitution on a single core is  $O(MN^2)$ , the cost might be reduced to only  $O(N)$  on  $M$  nodes (1 node per system) and  $N$  cores per node (1 core per solution component). Pseudocode and a visual proof of this is provided above, where layers of sequential operations are color-coded.

Consider also multi-grid (MG) schemes (for FDM [8]) and multi-scale basis sets (for regression [9]). It is well accepted in the uncertainty quantification (UQ) community that nature's physical processes are truly hierarchical, and it is often thought necessary to combine information across multiple grids and scales in order to create the highest fidelity model possible. While we further elaborate on this notion of hierarchy in natural processes in the subsequent subsection, we again provide a visual aid to highlight the computational hierarchy among coarser and finer grids as well as the hierarchy among smoother and sharper basis elements.



Consider the multi-level processing capabilities of a high-performance computing (HPC) cloud architecture [1, 2, 3]. Perhaps this is the most obvious hierarchy of a computational nature (and essentially a prerequisite for implementing any parallel codes). However, an uninitiated reader is likely to not be familiar with the language of: jobs, nodes, and cores. Without explaining the specifics of MPI [4] or SLURM [5], we provide the reader with the following additional context:

Multiple jobs can be run in parallel

Each job can be on many nodes

Each node is made of many cores

Such a pool of resources, coupled with such codes [6, 7], allow for a clever hacker to distribute the load of any non-sequential operations and achieve speedup.

For example, while the total cost of solving  $M$  different  $N \times N$  upper-triangular systems  $\mathbf{Rx} = \mathbf{y}$

## 1.2 Chemical Hierarchy

As promised, we now elaborate on the natural hierarchy [10] among “intrinsic” chemical properties such as: vibrational frequencies; internal energies; heat capacities, enthalpies, and entropies; Gibbs energies; forward, reverse, and equilibrium rate constants; and quantities like pressure, temperature, and species mass fractions. These are some key relationships from statistical thermodynamics and kinetics:

$$U = - \left( \frac{\partial}{\partial \beta} \ln Q \right)_V = -N \left( \left( \frac{\partial}{\partial \beta} \ln q_T \right)_V + \left( \frac{\partial}{\partial \beta} \ln q_R \right)_V + \left( \frac{\partial}{\partial \beta} \ln q_V \right)_V + \left( \frac{\partial}{\partial \beta} \ln q_E \right)_V \right)$$

$$U_T = \frac{3}{2} N k_B T = 3D \text{ Translational internal energy}$$

$$U_R = \begin{cases} N k_B T & \text{diatomic and linear polyatomic} \\ \frac{3}{2} N k_B T & \text{nonlinear polyatomic} \end{cases}$$

$$U_V = \frac{N h c \bar{\nu}}{e^{\beta h \bar{\nu}} - 1} = \text{Vibrational internal energy neglecting ZPE}$$

$$U_E = 0 = \text{Electronic internal energy for ground-state degeneracy}$$

$$C_V = \left( \frac{\partial U}{\partial T} \right)_V = -k_B \beta^2 \left( \frac{\partial U}{\partial \beta} \right)_V = \text{Heat capacity at constant volume}$$

$$S = \frac{U}{T} + k_B \ln Q = \text{Entropy}, \quad H = U + PV = \text{Enthalpy}$$

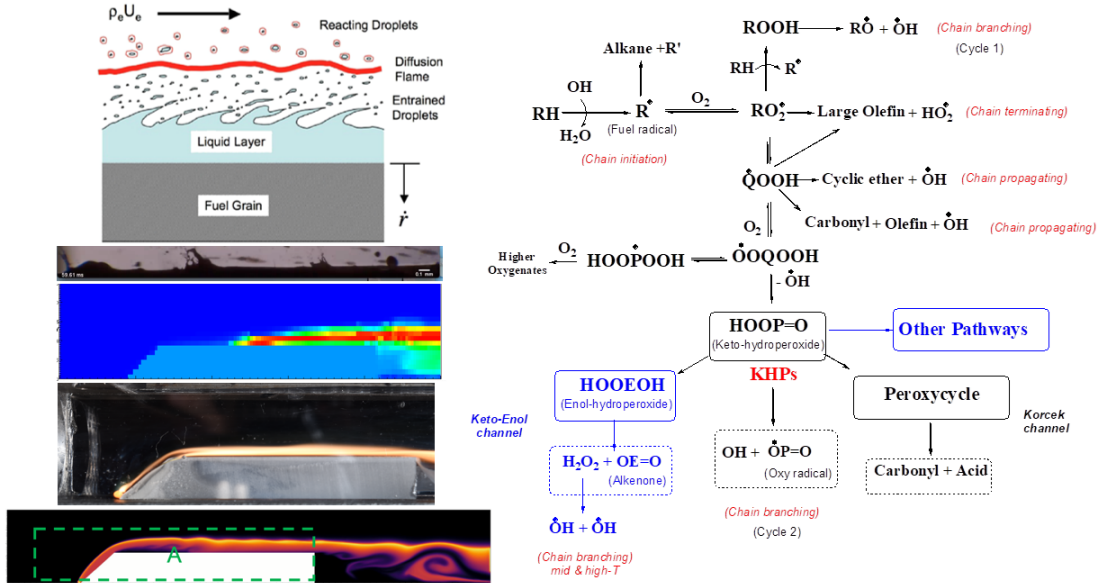
$$\Delta G = \Delta H - T \Delta S = \text{Gibbs free energy of reaction}$$

$$\Delta G^\ddagger = \Delta H^\ddagger - T \Delta S^\ddagger = \text{Gibbs free energy of activation}$$

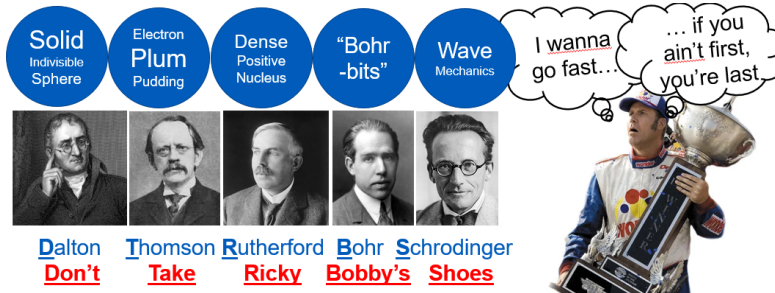
$$k_f = \frac{k_b T}{h} \exp \left( -\frac{\Delta G^\ddagger}{k_b T} \right), \quad k_r = \frac{k_f}{K}, \quad K = \exp \left( \frac{\Delta G}{k_b T} \right),$$

$$k_f = AT^b \exp \left( -\frac{E_a}{RT} \right),$$

Consider also cause and effect relationships (i.e.: causality). Networks of gas-phase chain-reactions are certainly causal as depicted below. Additionally, some processes, like turbulent combustion in hybrid rockets, are multi-phase. Meaning that the solid fuel must melt (and form shear-driven droplets) or sublime (directly to gas) in order to be injected into the propelling flow. This sequence of phase changes is causal too, and adds another layer of complexity to the problem space.



## 2 Problem



ear inverse problems which are both broadly tasks of interest in numerical PDEs. Before proceeding, it is worth noting that even the history and development of the atomic model was a hierarchical process. After Dalton declared the atom to be a solid, indivisible sphere, Thomson discovered the electron in an experiment with cathode ray tubes. But, Thomson's "Plum Pudding" model would also be debunked by Rutherford's gold foil experiment, detecting a dense, positive nucleus. Even Bohr's theory of orbit-like dynamics of electrons would be surpassed by Schrödinger's wave mechanical model. This can all easily be remembered [11] by the regionally famous mnemonic: D.T.R.B.S.

### 2.1 Toy Model: Particle in a Ring

Only some quantum-mechanical systems have nice, analytical solutions. For example, this can be done with the Schrödinger equation for a Hydrogen atom (or a Hydrogen-like ion), the Schrödinger equation for a quantum harmonic oscillator (QHO), and the Schrödinger equation for a particle in a box (PIB), ring (PIR), or lattice (PIL). In general, the Schrödinger equation can be represented as:  $\hat{H}\psi = E\psi$ , where  $\hat{H}$  is a Hamiltonian operator acting on a wavefunction  $\psi$ , and can be split into kinetic energy  $\hat{T}$  and potential energy  $\hat{V}$  components:

$$\hat{H}\psi = (\hat{T} + \hat{V})\psi$$

For the PIB, PIR, and PIL cases,  $\hat{V} = 0$  "inside" and  $\hat{V} = \infty$  "outside". So, each PDE is of the form:

$$-\frac{\hbar^2}{2m}\nabla^2\psi = E\psi$$

This contrasts with the QHO case (where  $\hat{V} = \frac{1}{2}m^2\omega^2\hat{x}^2$ ), and also contrasts with the H atom / H-like ion case (where  $\hat{V} = \frac{Ze^2}{4\pi\epsilon_0\hat{x}}$ ,  $m \neq m_e$ , and  $m = \frac{m_e m_{nuc}}{m_e + m_{nuc}}$ ). For PIR, specifically [12], we use the 1D Laplacian in angular coordinates  $\nabla^2 = \frac{1}{R^2}\frac{\partial^2}{\partial\theta^2}$ . And, it is well known that the analytical sequence of eigen-energies is:

$$E_n = \frac{n^2\hbar^2}{2mR^2}, \quad n = 0, \pm 1, \pm 2, \pm 3, \dots$$

However, when studying most quantum-mechanical systems, like performing ab initio electronic structure or vibrational frequency calculations, we often abandon analytics and resort to numerics. For instance, as we ascend in difficulty from modeling single electron systems to complex molecules, we meet the Kohn-Sham density-functional theory (KS-DFT) equations [13]:

$$\left( \hat{T} + \hat{V}_{ext} + e^2 \int \frac{\rho(r')}{|r - r'|} dr' + \hat{V}_{XC} \right) \psi = E\psi$$

which has a potential with external ( $\hat{V}_{ext}$ ), Coulombic ( $e^2 \int \frac{\rho(r')}{|r - r'|} dr'$ ) and exchange-correlational ( $\hat{V}_{XC}$ ) components. Ultimately, we hope our "new trick" could be applied to "QC/QQ" studies (see Section 5).

As previously aforementioned, the core result of this paper is showcasing an "old toy" with a "new trick". The following subsections connect traditional numerical methods for PDEs (i.e.: FDM/MG) to recursive Kronecker products with Pauli matrices. The particle in a ring model is discussed, but results are saved for Section 3. While this "old toy" is an eigenproblem, we emphasize that this "new trick" may also be applied to linear inverse problems which are both broadly tasks of interest in numerical PDEs. Before proceeding, it is worth noting that even the history and development of the atomic model was a hierarchical process. After Dalton declared the atom to be a solid, indivisible sphere, Thomson discovered the electron in an experiment with cathode ray tubes. But, Thomson's "Plum Pudding" model would also be debunked by Rutherford's gold foil experiment, detecting a dense, positive nucleus. Even Bohr's theory of orbit-like dynamics of electrons would be surpassed by Schrödinger's wave mechanical model. This can all easily be remembered [11] by the regionally famous mnemonic: D.T.R.B.S.

## 2.2 Traditional Methods: FDM, the Laplacian, and MG

We approach the traditional [14] formulation of  $\mathbf{L}^{(2^k)}$ , the 1D central difference Laplacian on a grid of  $2^k$  points with periodic boundary conditions (BCs), by first considering the limit definitions of the first and second derivatives of  $\psi$ :

$$\frac{\partial \psi}{\partial \theta} = \psi'(\theta) = \lim_{h \rightarrow 0} \frac{\psi(\theta + h) - \psi(\theta)}{h}$$

$$\frac{\partial^2 \psi}{\partial \theta^2} = \psi''(\theta) = \lim_{h \rightarrow 0} \frac{\psi'(\theta + h) - \psi'(\theta)}{h} = \lim_{h \rightarrow 0} \frac{\psi(\theta + 2h) - 2\psi(\theta + h) + \psi(\theta)}{h^2}$$

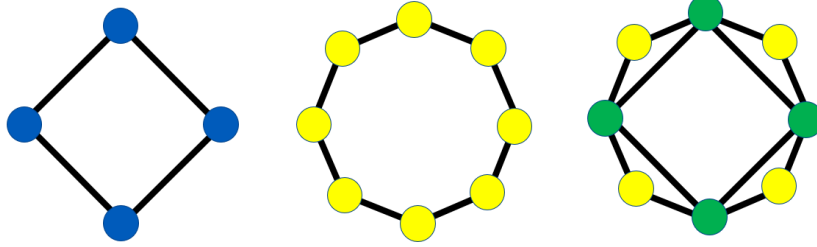
Consider also the limit as  $h \rightarrow 0$  of the coordinate transformation  $\theta \rightarrow \theta - h$ :

$$\lim_{h \rightarrow 0} \frac{\psi(\theta + 2h) - 2\psi(\theta + h) + \psi(\theta)}{h^2} = \lim_{h \rightarrow 0} \frac{\psi(\theta + h) - 2\psi(\theta) + \psi(\theta - h)}{h^2}$$

We have arrived at the central difference, and can construct  $\mathbf{L}^{(2^k)}$  such that:

$$\mathbf{L}^{(2^k)} = \frac{1}{[h(2^k)]^2} \begin{bmatrix} -2 & 1 & 0 & \dots & 1 \\ 1 & \ddots & \ddots & \ddots & \vdots \\ 0 & \ddots & \ddots & \ddots & 0 \\ \vdots & \ddots & \ddots & \ddots & 1 \\ 1 & \dots & 0 & 1 & -2 \end{bmatrix}, \quad h(2^k) = \frac{2\pi R}{2^k} = \text{Step Size for PIR}$$

Small refinements can be made to this matrix for alternative cases with Dirichlet or Neumann BCs.



A MG scheme (like a V-cycle) would additionally require relaxation matrices like  $\mathbf{R}^{(2^k)} = \mathbf{I}^{(2^k)} - \sigma \mathbf{L}^{(2^k)}$  with a “relaxation” factor  $\sigma$ . Additionally, they would require “prolongation” and “restriction” matrices:

$$(\mathbf{J}_{(2^k)}^{(2^{k+1})})^T = \mathbf{J}_{(2^{k+1})}^{(2^k)}$$

For example:

$$\mathbf{J}_{(2^2)}^{(2^3)} = \begin{bmatrix} 1 & 0 & 0 & 0 \\ 1/2 & 1/2 & 0 & 0 \\ 0 & 1 & 0 & 0 \\ 0 & 1/2 & 1/2 & 0 \\ 0 & 0 & 1 & 0 \\ 0 & 0 & 1/2 & 1/2 \\ 0 & 0 & 0 & 1 \\ 1/2 & 0 & 0 & 1/2 \end{bmatrix}$$

Think of the action of this matrix as “copying” and “interpolating”.

### 2.3 Novel Methods: Recursive Kronecker products with Pauli matrices

Furthermore, we use the conventions below:

$$\mathbf{M}_1^{(2^k)} = \bigotimes_{j=1}^k \left( \frac{\mathbf{X} + i\mathbf{Y}}{2} \right), \quad \mathbf{M}_2^{(2^k)} = \bigotimes_{j=1}^k \left( \frac{\mathbf{X} - i\mathbf{Y}}{2} \right), \quad \mathbf{M}_3^{(2^k)} = \bigotimes_{j=1}^k \left( \frac{\mathbf{I} + \mathbf{Z}}{2} \right), \quad \mathbf{M}_4^{(2^k)} = \bigotimes_{j=1}^k \left( \frac{\mathbf{I} - \mathbf{Z}}{2} \right)$$

Where  $\mathbf{I}$ ,  $\mathbf{X}$ ,  $\mathbf{Y}$ , and  $\mathbf{Z}$  are the Pauli matrices.

$$\mathbf{I} = \begin{bmatrix} 1 & 0 \\ 0 & 1 \end{bmatrix}, \quad \mathbf{X} = \begin{bmatrix} 0 & 1 \\ 1 & 0 \end{bmatrix}, \quad \mathbf{Y} = \begin{bmatrix} 0 & -i \\ i & 0 \end{bmatrix}, \quad \mathbf{Z} = \begin{bmatrix} 1 & 0 \\ 0 & -1 \end{bmatrix}$$

Consider the sequence defined by the recursion:

$$\mathbf{A}^{(2^2)} = 2\mathbf{I} \otimes \mathbf{I} - (\mathbf{I} + \mathbf{X}) \otimes \mathbf{X}, \quad \mathbf{A}^{(2^{k+1})} = \mathbf{I} \otimes \mathbf{A}^{(2^k)} + (\mathbf{I} - \mathbf{X}) \otimes \left( \mathbf{M}_1^{(2^k)} + \mathbf{M}_2^{(2^k)} \right) \quad (1)$$

This is exactly the sequence of graph Laplacians for the cycle graphs with  $2^k$  vertices, and has a direct relationship to the discrete Laplacian for our PIR problem:

$$-[h(2^k)]^2 \mathbf{L}^{(2^k)} = \mathbf{A}^{(2^k)}$$

Now, consider the sequence  $\mathbf{Q}_{(2^k)}^{(2^{k+1})}$  defined by:

$$\mathbf{Q}^{(2^{k+1})} = \langle \mathbf{0} | \otimes \mathbf{I}^{(2^{k-1})} \otimes \begin{bmatrix} 1 & 0 \\ 0 & 0 \\ 0 & 1 \\ 0 & 0 \end{bmatrix} + \langle \mathbf{1} | \otimes \mathbf{I}^{(2^{k-1})} \otimes \begin{bmatrix} 0 & 0 \\ 1 & 0 \\ 0 & 0 \\ 0 & 1 \end{bmatrix} \quad (2)$$

The diagram illustrates the factorization of a matrix  $J^{(2^{k+1})}$  into three components:  $Q^{(2^k)}$ ,  $B^{(2^k)}$ , and  $I^{(2^k)}$ . The matrix  $J^{(2^{k+1})}$  is shown as a large square divided into four quadrants. The top-left quadrant contains  $Q^{(2^k)}$ , the top-right quadrant contains  $(\gamma^{k+1})$ , the bottom-left quadrant contains  $(\gamma^k)$ , and the bottom-right quadrant contains  $B^{(2^k)}$ . The matrix  $Q^{(2^k)}$  is also labeled with its name above it. The matrix  $I^{(2^k)}$  is shown as a separate block to the right of the main matrix.

This allows us to factorize our “prolongation” and “restriction” matrices:

$$\mathbf{J}_{(2^{k+1})}^{(2^k)} = \left( |\mathbf{0}\rangle \otimes \mathbf{I}^{(2^k)} + |\mathbf{1}\rangle \otimes \mathbf{B}^{(2^k)} \right)^T \left( \mathbf{Q}^{(2^{k+1})} \right)^T = \mathbf{I}^{(2^{k-1})} \otimes \begin{bmatrix} 1 & 0 & 0 & 0 \\ 0 & 0 & 1 & 0 \end{bmatrix} + \left( \mathbf{B}^{(2^k)} \right)^T \left( \mathbf{I}^{(2^{k-1})} \otimes \begin{bmatrix} 0 & 1 & 0 & 0 \\ 0 & 0 & 0 & 1 \end{bmatrix} \right) \quad (3)$$

And to make our problem even easier, we can first solve:

$$\mathbf{C}^{(2^1)} = \begin{bmatrix} 1/2 & 1/2 \\ 0 & 1/2 \end{bmatrix}, \quad \mathbf{C}^{(2^{k+1})} = \mathbf{I} \otimes \mathbf{C}^{(2^k)} + \frac{1}{2} \left( \frac{\mathbf{X} + i\mathbf{Y}}{2} \right) \otimes \mathbf{M}_2^{(2^k)} \quad (4)$$

which is related to blocks of  $\mathbf{J}_{(2^k)}^{(2^{k+1})}$  prior to being permuted by  $\mathbf{Q}^{(2^{k+1})}$ . Specifically:

$$\mathbf{B}^{(2^{k+1})} = \mathbf{C}^{(2^{k+1})} + \frac{1}{2} \mathbf{M}_2^{(2^{k+1})} \quad (5)$$

### 3 Results

#### 3.1 Analytical Results

A closed form can be obtained by first approaching the “homogeneous” part:

$$\mathbf{A}_h^{(2^{k+1})} = \mathbf{I} \otimes \mathbf{A}_h^{(2^k)}, \quad \mathbf{A}_h^{(2^2)} = \mathbf{A}^{(2^2)}, \quad \mathbf{A}_h^{(2^{k+1})} = \mathbf{I}^{(2^{k-1})} \otimes \mathbf{A}_h^{(2^2)} \quad (6)$$

Then, we can also find a particular solution, and construct the full solution as:  $\mathbf{A}^{(2^{k+1})} = \mathbf{A}_h^{(2^{k+1})} + \mathbf{A}_p^{(2^{k+1})}$ :

$$\mathbf{A}_p^{(2^{k+1})} = \sum_{j=2}^k \left( \mathbf{I}^{(2^{j-2})} \otimes (\mathbf{I} - \mathbf{X}) \otimes \left( \mathbf{M}_1^{(2^{k-j+2})} + \mathbf{M}_2^{(2^{k-j+2})} \right) \right) \quad (7)$$

Leveraging the same technique, we find the solution for  $\mathbf{C}^{(2^{k+1})}$  to be:

$$\mathbf{C}^{(2^{k+1})} = \mathbf{I}^{(2^k)} \otimes \mathbf{C}^{(2^1)} + \frac{1}{2} \sum_{j=1}^k \left( \mathbf{I}^{(2^j)} \otimes \left( \frac{\mathbf{X} + i\mathbf{Y}}{2} \right) \otimes \mathbf{M}_2^{(2^{k-j})} \right) \quad (8)$$

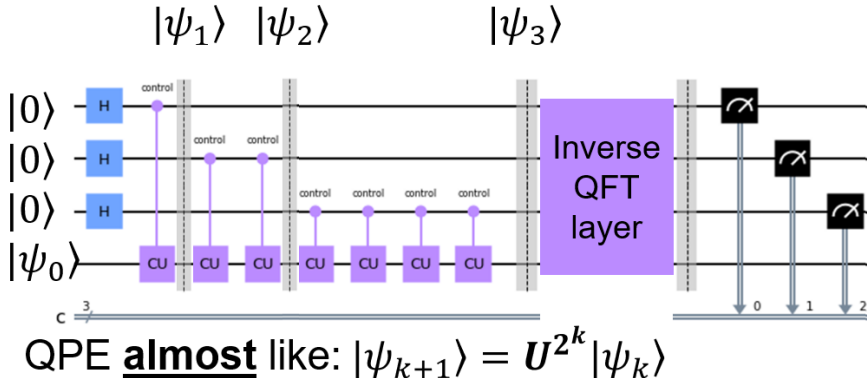
Thus:

$$\mathbf{B}^{(2^{k+1})} = \mathbf{I}^{(2^k)} \otimes \mathbf{C}^{(2^1)} + \frac{1}{2} \sum_{j=1}^k \left( \mathbf{I}^{(2^j)} \otimes \left( \frac{\mathbf{X} + i\mathbf{Y}}{2} \right) \otimes \mathbf{M}_2^{(2^{k-j})} \right) + \frac{1}{2} \mathbf{M}_2^{(2^{k+1})} \quad (9)$$

And, plugging this into the other equations above, we can obtain eventually obtain the Pauli decompositions of our “prolongation” and “restriction” matrices  $\mathbf{J}_{(2^k)}^{(2^{k+1})}$ .

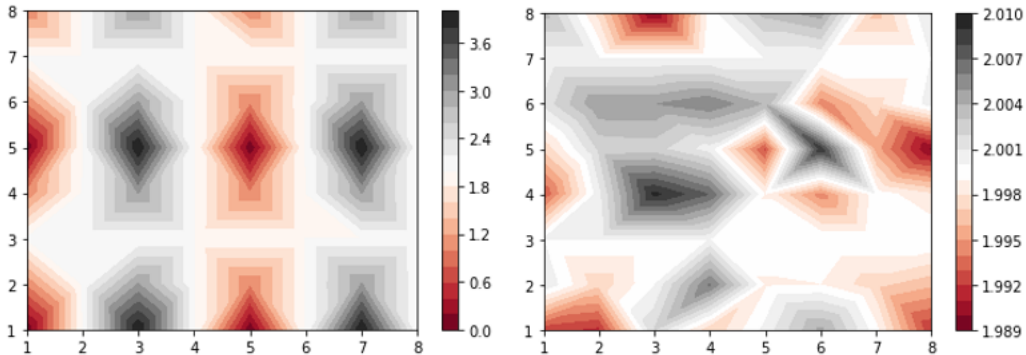
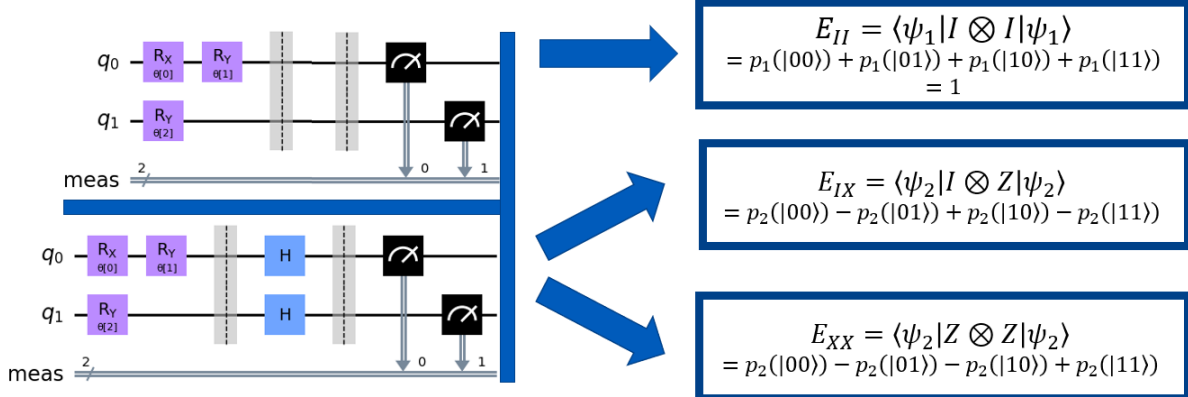
#### 3.2 Numerical Results

The purpose of using Pauli matrices was to steer us towards algorithms like quantum phase estimation (QPE) and the variational quantum eigensolver (VQE). QPE is akin to classical power iteration [15], and VQE [16] is tied to theorems like Rayleigh-Ritz and Courant-Fischer (CF). A QPE circuit, and the CF theorem are shown:



$$\max_{\psi^{(2^K)}, \dots, \psi^{(2^K)}_{n-1}} \min_{\psi^{(2^K)}_1, \dots, \psi^{(2^K)}_{n-1}} \langle \psi^{(2^K)} | A^{(2^K)} | \psi^{(2^K)} \rangle = E_n$$

Here, we choose to explore VQE due to its parallelizability across multiple quantum circuits. However, while we acknowledge that a parallelized and constrained gradient-descent implementation of CF would be ideal (in terms of cost) for obtaining all PIR energy levels, we present the reader with a simpler approach based on sampling. For each sample, Qiskit [17] was used different values to parameterize a different “guess” of an eigenvector (i.e.: a “trial state”). Each sample was parallelized across multiple quantum circuit simulations, and each quantum circuit simulation was executed on a different classical node. After analysis, some experiments can be repeated on real IBM quantum hardware. Computing expectation values from the probabilities measured (see Section 4.2) is a strictly classical task (i.e.: post-processing), but is also parallelizable. A summary table is provided below along with a diagram for the parallel VQE steps.



	Eigenvalues	$\theta_1$	$\theta_2$	$\theta_3$
Simulator	0	0	$\pi/2$	$\pi/2$
	4	0	$7\pi/2$	$\pi/2$
	2	$\pi/2$	0	$7\pi/2$
	2	$7\pi/2$	0	$7\pi/2$
Hardware		0	$\pi/2$	$\pi/2$
		0	$7\pi/2$	$\pi/2$
		$\pi/2$	0	$7\pi/2$
		$7\pi/2$	0	$7\pi/2$

Blank table cells indicate experiments to be repeated on IBM Eagle processors (with 127 qubits). Parallelization can occur across: “ibm\_brisbane”, “ibm\_osaka”, and “ibm\_kyoto” [18]. Supporting code and simulator results are provided here: <https://github.com/ajbecerr/PIR/tree/main>

## 4 Discussion

### 4.1 Analytical Discussion

The main point of our “new trick” is that it avoids the need for diagonalization. Is this good or bad? In truth, our “new trick” and diagonalization both have pros and cons.

Not all matrices are diagonalizable. So, in general that would favor our “new trick”, but the PIR case is diagonalizable by the quantum Fourier transform (QFT). Once diagonalized, linear systems problems become easier, and eigenproblems become completely trivial. Additionally, we can “truncate” certain parts of the “spectrum” that we do not want.

However, we claim that it is also more costly to diagonalize. And, by proceeding directly, we specifically claim that we can save both time and hardware resources in “fully quantum” or a hybrid classical-quantum routine (with QPE or VQE variants). Simply, by avoiding both classical pre-processing time and resources (even with an fast-fourier transform, i.e.: FFT), and also by avoiding the need to “transpile” costly (and maybe even noisy!) QFT gate layers onto real quantum hardware, we expect our direct Pauli decomposition of the Hamiltonian (via recursive Kronecker products) to perform better in a wide variety of scenarios. These comparisons can be left to future work.

Notably, a diagonalized version of our “new trick”:

$$\mathbf{D}^{(2^2)} = \left(\mathbf{U}_{QFT}^{(2^2)}\right)^\dagger \mathbf{A}^{(2^2)} \mathbf{U}_{QFT}^{(2^2)}, \quad \mathbf{D}^{(2^{k+1})} = \left(\mathbf{U}_{QFT}^{(2^{k+1})}\right)^\dagger \mathbf{A}^{(2^{k+1})} \mathbf{U}_{QFT}^{(2^{k+1})}$$

cannot be solved “nicely” in this case because there is not a “nice” recursive Kronecker decomp. for  $\mathbf{U}_{QFT}^{(2^k)}$ :

$$\mathbf{U}_{QFT}^{(2^{k+1})} \neq \mathbf{U}_{QFT}^{(2^1)} \otimes \mathbf{U}_{QFT}^{(2^k)}$$

### 4.2 Numerical Discussion

In general, expectations can be computed with probabilities measured from a 2-qubit state using facts like:

$$\mathbf{I} \otimes \mathbf{I} = (|\mathbf{0}\rangle\langle\mathbf{0}| + |\mathbf{1}\rangle\langle\mathbf{1}|) \otimes (|\mathbf{0}\rangle\langle\mathbf{0}| + |\mathbf{1}\rangle\langle\mathbf{1}|)$$

$$\mathbf{I} \otimes \mathbf{X} = (\mathbf{H}\mathbf{H}) \otimes (\mathbf{H}\mathbf{Z}\mathbf{H}) = (\mathbf{H} \otimes \mathbf{H}) ((|\mathbf{0}\rangle\langle\mathbf{0}| + |\mathbf{1}\rangle\langle\mathbf{1}|) \otimes (|\mathbf{0}\rangle\langle\mathbf{0}| - |\mathbf{1}\rangle\langle\mathbf{1}|)) (\mathbf{H} \otimes \mathbf{H})$$

$$\mathbf{X} \otimes \mathbf{X} = (\mathbf{H}\mathbf{Z}\mathbf{H}) \otimes (\mathbf{H}\mathbf{Z}\mathbf{H}) = (\mathbf{H} \otimes \mathbf{H}) ((|\mathbf{0}\rangle\langle\mathbf{0}| - |\mathbf{1}\rangle\langle\mathbf{1}|) \otimes (|\mathbf{0}\rangle\langle\mathbf{0}| - |\mathbf{1}\rangle\langle\mathbf{1}|)) (\mathbf{H} \otimes \mathbf{H})$$

For preparing the trial states, our quantum ansätze works for the PIR case because:

$$(\mathbf{R}_y(\pi/2) \otimes \mathbf{R}_y(\pi/2)) |\mathbf{0}\mathbf{0}\rangle = 1/2 [1 \ 1 \ 1 \ 1]^T, \quad (\mathbf{R}_y(\pi/2) \otimes \mathbf{R}_y(-\pi/2)) |\mathbf{0}\mathbf{0}\rangle = 1/2 [1 \ -1 \ 1 \ -1]^T$$

$$(\mathbf{R}_y(-\pi/2) \otimes \mathbf{R}_x(\pi/2)) |\mathbf{0}\mathbf{0}\rangle = 1/2 [1 \ -i \ -1 \ i]^T, \quad (\mathbf{R}_y(-\pi/2) \otimes \mathbf{R}_x(-\pi/2)) |\mathbf{0}\mathbf{0}\rangle = 1/2 [1 \ i \ -1 \ -i]^T$$

In other words, the parameterized space “covers” the eigenvectors. Here, we define:

$$\mathbf{R}_y(2\theta) = \begin{bmatrix} \cos \theta & -\sin \theta \\ \sin \theta & \cos \theta \end{bmatrix}, \quad \mathbf{R}_x(2\theta) = \begin{bmatrix} \cos \theta & -i \sin \theta \\ -i \sin \theta & \cos \theta \end{bmatrix}, \quad \mathbf{H} = \frac{1}{\sqrt{2}} \begin{bmatrix} 1 & 1 \\ 1 & -1 \end{bmatrix}$$

And, in total, for each trial, we compute in parallel (with 2 different quantum circuits and 3 classical nodes):

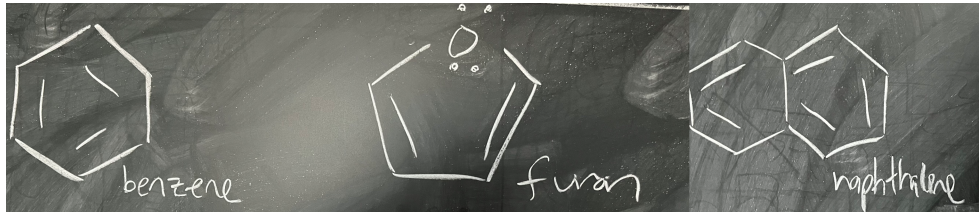
$$\langle \mathbf{0}\mathbf{0} | \mathbf{U}^\dagger(\theta_1, \theta_2, \theta_3) \mathbf{A}^{(2^2)} \mathbf{U}(\theta_1, \theta_2, \theta_3) | \mathbf{0}\mathbf{0} \rangle = \langle \psi(\theta_1, \theta_2, \theta_3) | \mathbf{A}^{(2^2)} | \psi(\theta_1, \theta_2, \theta_3) \rangle$$

$$= 2\langle \psi(\theta_1, \theta_2, \theta_3) | (\mathbf{I} \otimes \mathbf{I}) | \psi(\theta_1, \theta_2, \theta_3) \rangle - \langle \psi(\theta_1, \theta_2, \theta_3) | (\mathbf{I} \otimes \mathbf{X}) | \psi(\theta_1, \theta_2, \theta_3) \rangle - \langle \psi(\theta_1, \theta_2, \theta_3) | (\mathbf{X} \otimes \mathbf{X}) | \psi(\theta_1, \theta_2, \theta_3) \rangle$$

$$= 2\langle \psi_1(\theta_1, \theta_2, \theta_3) | (\mathbf{I} \otimes \mathbf{I}) | \psi_1(\theta_1, \theta_2, \theta_3) \rangle - \langle \psi_2(\theta_1, \theta_2, \theta_3) | (\mathbf{I} \otimes \mathbf{Z}) | \psi_2(\theta_1, \theta_2, \theta_3) \rangle - \langle \psi_2(\theta_1, \theta_2, \theta_3) | (\mathbf{Z} \otimes \mathbf{Z}) | \psi_2(\theta_1, \theta_2, \theta_3) \rangle$$

### 4.3 Broader Discussion

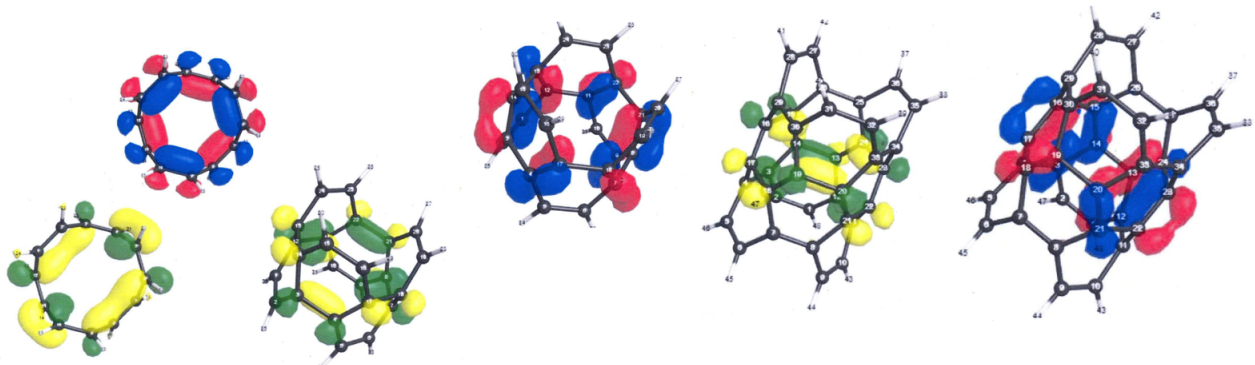
While we introduced PIR as simply an “old toy”, in truth, it has value in modeling some molecules like “aromatic” ones. This does not mean molecules which have a smell. “Aromaticity” is a property related to “Hückel’s rule” [19]. Planar molecules having  $(4n + 2) \pi$ -electrons in a delocalized ring of overlapping  $p$ -orbitals are considered to be “aromatic”. Examples include PAHs (relevant in soot modeling) and more:



Hückel, who treated molecular orbitals (MOs) as linear combinations of atomic orbitals (AOs), predicted the energy levels of benzene ( $C_6H_6$ ) as shown below where the multiplicities in eigen-energies are explained by the patterns in “bonding MOs” and “anti-bonding MOs”.



Now, consider what would happen if we took a PIR problem and modified the domain by allowing the ring to revolve around itself? We would get a particle in the boundary of a sphere (essentially, a higher-dimensional PIR). Are there any molecules like this? Of course! The common examples provided are types of “fullerenes” like  $C_{60}$  (the “buckyball”, i.e.: “buckminsterfullerene”). But, surely we can think of even more applications in a similar space of materials. What if we instead “extruded” our ring to make a “tube”? Then, we could get something that looks like a “single-walled carbon nanotube” (SWNT). Computational studies of SWNTs typically seek to determine the “band gap energy” by computing the highest- and lowest- occupied MOs. This can be done for a variety of tube diameters and lengths in order to determine the optimal geometric structure for nanoscale semiconductor applications:



Furthermore, we once again call back to the notion that in order to perform detailed chemical kinetics computations (like for reacting flow applications), we sometimes require ab initio estimates of thermodynamic properties (generally obtained through KS-DFT, a PDE similar to, but more complex than PIR). In cases where there is a lack of quality experimental data, this is particularly needed to establish realistic values of model parameters. Quality thermodynamic inputs are essential to obtain quality kinetic outputs.

## 5 Conclusion

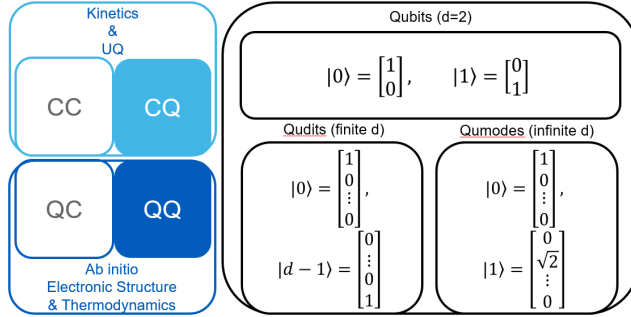
Clearly, since the 2-dimensional Laplacian can be discretized as:

$$\mathbf{L}_{2D}^{(2^k)} = \mathbf{L}_{1D}^{(2^k)} \otimes \mathbf{I}^{(2^k)} + \mathbf{I}^{(2^k)} \otimes \mathbf{L}_{1D}^{(2^k)}$$

And, since we can decompose **CNOT** and **CU** gates like:

$$\begin{aligned}\mathbf{CNOT}_{1,0} &= \begin{bmatrix} 1 & 0 & 0 & 0 \\ 0 & 1 & 0 & 0 \\ 0 & 0 & 0 & 1 \\ 0 & 0 & 1 & 0 \end{bmatrix} = \left(\frac{\mathbf{I} + \mathbf{Z}}{2}\right) \otimes \mathbf{I} + \left(\frac{\mathbf{I} - \mathbf{Z}}{2}\right) \otimes \mathbf{X} \\ \mathbf{CU}_{0,3} &= \mathbf{I} \otimes \mathbf{I} \otimes \mathbf{I} \otimes \left(\frac{\mathbf{I} + \mathbf{Z}}{2}\right) + \mathbf{U} \otimes \mathbf{I} \otimes \mathbf{I} \otimes \left(\frac{\mathbf{I} - \mathbf{Z}}{2}\right) \\ \mathbf{CU}_{1,3} &= \mathbf{I} \otimes \mathbf{I} \otimes \left(\frac{\mathbf{I} + \mathbf{Z}}{2}\right) \otimes \mathbf{I} + \mathbf{U} \otimes \mathbf{I} \otimes \left(\frac{\mathbf{I} - \mathbf{Z}}{2}\right) \otimes \mathbf{I} \\ \mathbf{CU}_{2,3} &= \mathbf{I} \otimes \left(\frac{\mathbf{I} + \mathbf{Z}}{2}\right) \otimes \mathbf{I} \otimes \mathbf{I} + \mathbf{U} \otimes \left(\frac{\mathbf{I} - \mathbf{Z}}{2}\right) \otimes \mathbf{I} \otimes \mathbf{I}\end{aligned}$$

there is a lot of potential to build on our results in the future. Ultimately, we have shown the consistency of our “new trick” as well as some potential uses for this “old toy”. And, we have covered a lot of ground in the computational chemistry space. So, now it is time to reflect on our hierarchical explorations by explaining how they fit into a popular new paradigm:



The “CC/CQ” + “QC/QQ” paradigm delineates between classical and quantum problems (in reference to the first letter) as well as classical and quantum solutions (in reference to the second letter). Our “old toy” - PIR - is a quantum problem, and fits within the “QC/QQ” boxes. Our “new trick” is not inherently a classical or quantum solution method, but rather a “quantum-inspired” one. Meaning that it either can be used in a strictly “QQ” context (with quantum hardware), or it can be used in a strictly “QC” context (with classical hardware). Also, as done here, both classical and quantum hardware can be simultaneously used (since VQE is a hybrid method). There has been a significant rise in the development of a variety of highly-specialized classical computational architectures including new kinds of CPUs, GPUs [20], and TPUs [21] (as well a variety of highly-specialized quantum computational architectures including new kinds of qubits, qudits [22], and qumodes [23]). Each may be “better suited” for something different (ex: tensor networks, machine learning (ML) approaches [24], etc.), although sometimes it may be difficult to benchmark the performance differences (ex: FLOPs v.s. CLOPs) [25]. Nevertheless, for now, in the noisy intermediate-scale quantum (NISQ) era [26], classical hardware still reigns supreme. Quantum computer-aided design (QCAD) might be able to accelerate the path towards full-scale, fault-tolerant quantum devices [27]. However, Moore’s “law” is now said (by some [28]) to be “dead-er” than Moore himself. And with no “quantum revolution” in sight, how are we supposed to approach answering the hard UQ questions of today? How does one know if an intracatalytic hydrogen atom transfer (“CHAT”) is truly “catalytic” (and not just a “HAT”) [29]? How does one know how much “5-Methoxy Peach Pie” you should eat [30]? We still do not claim to know, nor do we claim to have a solution (or a use) for higher-degree versions of our trick:  $\mathbf{F}^{(2^{k+2})} = \mathbf{G}_1^{(2^1)} \otimes \mathbf{F}^{(2^{k+1})} + \mathbf{G}_2^{(2^2)} \otimes \mathbf{F}^{(2^k)}$ . We just strive for “pretty mathematics” [31].

## 6 Division of work

I attest that I synthesized the entire project.

All codes and visuals were made from scratch.

While most artwork is entirely original, some images (or some likenesses) appearing in visuals were sourced internally (from collaborators) or occasionally externally (in the cases of Slurms McKenzie and Ricky Bobby).

Hundreds of parameterized quantum circuit jobs were run in parallel on LLNL Quartz, and optimization plots were post-processed in a Jupyter Notebook created on Tufts HPC.

This direction of ideas (quantum-inspired FDM) was a mainly product of collaboration and innovation with Eric A. Walker, who formulated a discrete KS-DFT problem for CO oxidation with an Ru catalyst suitable for a Trotterized QPE algorithm.

Here, my “new trick” is recycled for discrete PIR (with a parallel VQE instead of a serial QPE), and a larger context is built up around MG methods (which also can employ my “new trick”).

Abani Patra helped shape parallelization + MG + UQ discussions.

## References

- [1] [https://www.buffalo.edu/CCR/support/research\\_facilities/ub-hpc/academic-hardware\\_specs.html](https://www.buffalo.edu/CCR/support/research_facilities/ub-hpc/academic-hardware_specs.html), “Academic compute partitions hardware specs,” *UB CCR*, 2023.
- [2] [https://it.tufts.edu/high-performance computing](https://it.tufts.edu/high-performance-computing), “High performance computing,” *Tufts TTS*, 2023.
- [3] <https://hpc.llnl.gov/hardware/compute-platforms/quartz>, “Llnl quartz,” *Livemore Computing*, 2023.
- [4] <https://hpc-tutorials.llnl.gov/mpi/>, “Message passing interface (mpi),” *Blaise Barney, Lawrence Livermore National Laboratory (LLNL)*, 2023.
- [5] <https://hpc.llnl.gov/banks-jobs/running-jobs/slurm>, “Slurm tutorial (formerly slurm and moab),” *Livemore Computing*, 2023.
- [6] <https://ablate.dev/>, “Ablate: Ablative boundary layers at the exascale,” *UB CHREST*, 2023.
- [7] <https://www.mcs.anl.gov/petsc/petsc-3.6/docs/manual.pdf>, “PetSc users manual,” *Argonne National Laboratory (ANL) Mathematics and Computer Science Division*, 2023.
- [8] B. Henson and McCormick, “A multigrid tutorial,” *SIAM*, 2000.
- [9] <https://arxiv.org/abs/2102.07068>, “A forward backward greedy approach for sparse multiscale learning,” *Prashant Shekhar, Abani Patra*, 2021.
- [10] Engel and Reid, “Thermodynamics, statistical thermodynamics, and kinetics (3e),” *Pearson*, 2013.
- [11] J. Flick, “Talladega nights: The ballad of ricky bobby,” *Liverpool HS*, 2017.
- [12] M. Solà and F. M. Bickelhaupt, “Particle on a ring model for teaching the origin of the aromatic stabilization energy and the hückel and baird rules,” *ACS Journal of Chemical Education*, 2022.
- [13] Bylaska, Holst, and Weare, “Adaptive finite element method for solving the exact kohn-sham equation of density functional theory,” *ACS J. Chem. Theory Comput.*, 2008.
- [14] Demanet and White, “18.336/6.335 fast methods for partial differential and integral equations,” *MIT*, 2013.

- [15] C. P. II, “Lecture 11: Application 2 of qft / qpe: Quantum chemistry,” *University of Cambridge*, 2023.
- [16] P. J. L. (Tufts) and A. A.-G. Z. Computing), “A variational eigenvalue solver on a quantum processor,” *arXiv*, 2013.
- [17] Q. is the open-source toolkit for useful quantum, “<https://www.ibm.com/quantum/qiskit>,” *IBM Quantum Computing*, 2023.
- [18] I. Q. P. C. Resources, “<https://quantum.ibm.com/services/resources>,” *IBM Quantum Computing*, 2023.
- [19] Bruice, “Organic chemistry (8e),” *Pearson*, 2017.
- [20] B. Carreño and L. Howes, “The rise of gpu computing in science,” *EMBL*, 2023.
- [21] A. A. development with Google Cloud TPUs, “<https://cloud.google.com/tpu>,” *Google*, 2023.
- [22] G. Alonso, “Qutrits and quantum algorithms,” *Xanadu Penny Lane*, 2023.
- [23] I. to quantum photonics, “<https://strawberryfields.ai/photonics/concepts/photonics.html>,” *Xanadu Strawberry Fields*, 2023.
- [24] Q. M. L. overview, “<https://qiskit.org/ecosystem/machine-learning/>,” *IBM*, 2023.
- [25] D. quantum performance: more qubits higher Quantum Volume and now a proper measure of speed, “<https://research.ibm.com/blog/circuit-layer-operations-per-second>,” *IBM*, 2023.
- [26] N. I.-S. Q. algorithms, “[https://indico.cern.ch/event/1015866/contributions/4391136/attachments/2283322/3880374/nis\\_CERN](https://indico.cern.ch/event/1015866/contributions/4391136/attachments/2283322/3880374/nis_CERN)”, 2021.
- [27] A. Aspuru-Guzik, “Designing quantum hardware with quantum computers,” *Substack*, 2020.
- [28] W. Witkowski, “Moore’s law’s dead: Nvidia ceo jensen huang says in justifying gaming-card price hike,” *Marketwatch*, 2022.
- [29] R. Asatryan, “Intramolecular catalytic hydrogen atom transfer (chat),” *TBD*, 2024 (In preparation).
- [30] H. Morris, “Sihkal: Shulgins i have known and loved,” *Vice*, 2010.
- [31] P. Dirac, “Pretty mathematics,” *Springer*, 1982.